



## Electrocatalytic properties of Pt–Bi electrodes towards the electro-oxidation of formic acid

JELENA D. LOVIĆ<sup>#</sup>, DUŠAN V. TRIPKOVIĆ<sup>#</sup>, KSENIJA Đ. POPOVIĆ<sup>#</sup>,  
VLADISLAVA M. JOVANOVIĆ<sup>#</sup> and AMALIJA V. TRIPKOVIĆ<sup>\*\*</sup>

*ICTM – Institute of Electrochemistry, University of Belgrade, Njegoševa 12, P. O. Box 473,  
11000 Belgrade, Serbia*

(Received 12 October, revised 16 November 2012)

**Abstract:** Formic acid oxidation was studied on two Pt–Bi catalysts, *i.e.*, Pt<sub>2</sub>Bi and polycrystalline Pt modified by irreversible adsorbed Bi (Pt/Bi<sub>irr</sub>) in order to establish the difference between the effects of Bi<sub>irr</sub> and Bi in the alloyed state. The results were compared to pure Pt. It was found that both bimetallic catalysts were more active than Pt with the onset potentials shifted to more negative values and the currents at 0.0 V *vs.* saturated calomel electrode (under steady state conditions) improved by up to two order of magnitude. The origin of the high activity and stability of Pt<sub>2</sub>Bi was increased selectivity toward formic acid dehydrogenation caused by the ensemble and electronic effects and suppression of Bi leaching from the surface during formic acid oxidation. However, although Pt/Bi<sub>irr</sub> also showed remarkable initial activity compared to pure Pt, dissolution of Bi was not suppressed and poisoning of the electrode surface induced by the dehydration path was observed. Comparison of the initial quasi-steady state and potentiodynamic results obtained for these two Pt–Bi catalysts revealed that the electronic effect, existing only in the alloy, contributed to the earlier start of the reaction, while the maximum current density was determined by the ensemble effect.

**Keywords:** formic acid; electrochemical oxidation; Pt<sub>2</sub>Bi catalyst; Pt/Bi<sub>irr</sub> catalyst; fuel cell.

### INTRODUCTION

The electrocatalytic oxidation of small organic molecules, such as methanol, ethanol and formic acid, has been extensively studied because such molecules can potentially be used as fuel in fuel cell applications.<sup>1</sup> Pt is an excellent catalyst for the dehydrogenation of small organic molecules but, on the other hand, has several significant disadvantages, such as high cost and extreme susceptibility to

\* Corresponding author. E-mail: amalija@tmf.bg.ac.rs

# Serbian Chemical Society member.

doi: 10.2298/JSC121012138L

poisoning by CO. To improve its catalyst performance and minimize its amount in catalysts, Pt has been modified by the addition of other metals, such as Ru, Rh, Pd, Sn, Pb, etc.<sup>2–5</sup>

The electrochemical oxidation of formic acid has been comprehensively investigated as the anodic reaction in direct formic acid fuel cells (DFAFC) and as a model reaction important for the understanding the electro-oxidation of other small organic molecules.<sup>6,7</sup> Mechanistic studies of formic acid electro-oxidation suggested that the reaction on Pt proceeds through two parallel paths:<sup>8</sup> dehydrogenation with direct oxidation to CO<sub>2</sub> and a path consisting of a dehydration step, to yield water and adsorbed CO (CO<sub>ad</sub>), as a poisoning intermediate, and the subsequent oxidation of CO<sub>ad</sub> to CO<sub>2</sub>. Since the potential of CO<sub>ad</sub> formation is lower than the dehydrogenation potential, the poison remains on electrode surfaces until it is oxidized by oxygen-containing species at positive potentials.<sup>9</sup> Thus, the Pt atoms covered with poison are not available for dehydrogenation and the catalytic efficiency of the Pt surface decreases.

Therefore, practical application of Pt for formic acid oxidation requires some modification of the surface. This is commonly realized by alloying or by alteration of the Pt surface with adsorbed foreign metals in amounts less than a full monolayer. As the CO<sub>ad</sub> poison require an ensemble of Pt surface atoms to adsorb on, modification of the local distribution of surface domains is achieved by adsorption of different ad-atoms, such as Bi. Irreversibly adsorbed Bi,<sup>10–13</sup> inhibits poison formation and simultaneously enhances dehydrogenation,<sup>13</sup> *i.e.*, this modification is an efficient way to hinder the dehydration path (CO-intermediate pathway) in favor of the direct path.<sup>14</sup> This increased selectivity for dehydrogenation has been proposed as an “ensemble effect”<sup>15,16</sup> in which the adsorbed Bi divides the Pt surface into small domains where only dehydrogenation can occur. A correlation between ensemble size and formic acid oxidation activity was also established.<sup>17</sup> According to literature data, the activity of a Pt catalyst modified with Bi depends on the shape of the Pt nanocrystals,<sup>18</sup> the size of the particles<sup>19</sup> and Pt catalyst loading.<sup>14</sup>

Ordered intermetallic PtBi or PtBi<sub>2</sub> alloys<sup>20–23</sup> and PtBi alloy nanoparticles<sup>24–29</sup> were proposed as good catalysts for formic acid oxidation. The onset potential of the reaction is significantly shifted to more negative values (by over 300 mV) and the current density is remarkably enhanced over the whole potential range compared to Pt.<sup>30</sup> Moreover, the PtBi surface appears to have a considerably lower sensitivity to poisoning by CO according to DEMS,<sup>22,30</sup> FTIR<sup>22,31</sup> and DFT calculations.<sup>22,23,32</sup> The origin of its catalytic activity was related to electronic effects. The formation of the PtBi ordered intermetallic phase results in a charge redistribution, enhancing the affinity of PtBi for formic acid adsorption and producing surface oxides at low potentials,<sup>25,33</sup> as well as to geometric effects reducing the affinity for CO poisoning. In addition, the excellent catalytic



properties of PtBi nanoparticles can be attributed to the occurrence of the ensemble effect on the nanoscale level.<sup>29</sup>

In previous studies, the oxidation of formic acid was investigated on single phase PtBi alloy,<sup>34</sup> as well as on Pt<sub>2</sub>Bi catalyst, a two-phase material consisting of PtBi alloy and pure Pt.<sup>35</sup> A huge increase in catalytic activity on the PtBi electrode relative to polycrystalline Pt was observed and discussed in terms of electrochemically detected UPD phenomena of Bi re-adsorbed on Pt. Additionally, based on the analysis of X-ray photoelectron spectra, it was proposed that the bifunctional action of hydroxylated Bi species may contribute to the enhanced activity of PtBi alloys.<sup>34</sup> Pt<sub>2</sub>Bi was found to be powerful catalyst for formic acid oxidation, exhibiting high activity and stability. The high activity originates from the fact that formic acid oxidation proceeds entirely through the dehydrogenation path, while the high stability of Pt<sub>2</sub>Bi surface is induced by the suppression of Bi leaching in the presence of formic acid.<sup>35</sup> It is difficult to separate the contributions of the ensemble and the electronic effect since both of them could be present in the Pt–Bi surfaces.

In the present study, formic acid oxidation was studied on two types of Pt–Bi surfaces: polycrystalline Pt modified by irreversibly adsorbed Bi (designated as Pt/Bi<sub>irr</sub>) and a Pt<sub>2</sub>Bi catalyst. In order to investigate the promotional role of Bi in formic acid oxidation, as well as the difference between the effect of irreversibly adsorbed Bi and Bi in the alloyed state, Pt was modified with  $\approx 30\%$  Bi<sub>irr</sub>, which correspond to the nominal content of Bi in the Pt<sub>2</sub>Bi catalyst. The comparative investigation based on the effects influencing the catalytic properties of these electrodes enabled a better understanding of the difference in the activities between the Pt<sub>2</sub>Bi catalyst and the Bi<sub>irr</sub> modified Pt.

## EXPERIMENTAL

Polycrystalline Pt and Pt<sub>2</sub>Bi electrodes in the form of discs were used in this study. Pt<sub>2</sub>Bi catalyst was prepared and characterized at the Institute of Catalysis and Surface Chemistry, Polish Academy of Sciences, Krakow, Poland.<sup>35</sup> Briefly, the catalyst was fabricated by melting the pure elements in an inert atmosphere in the proportion of Bi to Pt of 1:2 and characterized by X-ray diffraction (XRD) analysis. Diffraction pattern for Pt<sub>2</sub>Bi sample revealed two crystal phases: platinum (*fcc*) and platinum bismuth PtBi (*hcp*). The phase composition of the sample was calculated using the Rietveld refinement as 45 % and 55 % for Pt and PtBi phases, respectively.

Prior to each experiment, the electrodes were mirror polished (1–0.05  $\mu\text{m}$  Buehler alumina). The surfaces were rinsed with high purity water (Millipore, 18  $\text{M}\Omega\text{ cm}$  resistivity), sonicated for 2–3 min and rinsed again with ultrapure water.

All experiments were performed on the as-prepared catalysts. Three-compartment electrochemical glass cells with a Pt wire as the counter electrode and a saturated calomel electrode (SCE) as the reference electrode were used. All the potentials are expressed on the SCE scale. The electrolyte containing 0.1 M H<sub>2</sub>SO<sub>4</sub> as a supporting electrolyte and 0.125 M HCOOH was prepared with high purity water and *p.a.* grade chemicals (Merck). The electrolyte was de-aerated by bubbling with nitrogen. Upon addition of HCOOH at –0.20 V,



potentiodynamic ( $v = 50 \text{ mV s}^{-1}$ ), quasi steady-state measurements ( $v = 1 \text{ mV s}^{-1}$ ) or chronoamperometric measurements were performed. The electrode was rotating at 2000 rpm in all the experiments.

Modification of the Pt electrode was performed from  $1 \times 10^{-5} \text{ M Bi}_2\text{O}_3$  in  $0.1 \text{ M H}_2\text{SO}_4$  at the open circuit potential during 45 s. After modification, the electrode (denoted Pt/Bi<sub>irr</sub>) was rinsed with water and transferred into a cell containing the supporting electrolyte. The fraction of the sites covered by Bi was estimated from the decrease in the charge for the desorption of hydrogen, assuming a charge of  $210 \mu\text{C cm}^{-2}$  for hydrogen monolayer adsorption.

The real surface area of all the as-prepared catalysts was calculated from CO stripping voltammetry. For the CO stripping measurements, pure CO was bubbled through the electrolyte for 20 min while keeping the electrode potential at  $-0.20 \text{ V vs. SCE}$ . After purging the electrolyte by N<sub>2</sub> for 30 min to eliminate the dissolved CO, the adsorbed CO was oxidized in an anodic scan at  $50 \text{ mV s}^{-1}$ . Two subsequent voltammograms were recorded to verify the completeness of the CO oxidation. The real surface area of all the employed electrodes was estimated by calculation of the charge from the CO<sub>ad</sub> stripping voltammograms corrected for background currents. Assuming a charge of  $420 \mu\text{C cm}^{-2}$  for a CO monolayer adsorption on the Pt electrode, a roughness factor of  $1.4 \pm 0.1$  was estimated. The real surface area of the Pt<sub>2</sub>Bi electrode was estimated assuming the same roughness factor as for the Pt electrode, which is to be expected since both electrodes were polished in the same way. The specific activity of Pt and Pt<sub>2</sub>Bi electrodes for formic acid oxidation were normalized using these values of the surface area.

The experiments were conducted at  $295 \pm 0.5 \text{ K}$  employing a VoltaLab PGZ 402 (Radiometer Analytical, Lyon, France).

## RESULTS AND DISCUSSION

### *Electrochemical characterization*

The initial voltammograms of the as-prepared Pt and Pt/Bi<sub>irr</sub> catalysts are presented in Fig. 1. The cyclic voltammogram for the polycrystalline Pt electrode is characterized by a defined region of hydrogen adsorption/desorption ( $E < 0.05 \text{ V}$ ), separated by a double layer from the region of surface oxide formation ( $E > 0.45 \text{ V}$ ). The absence of well-developed peaks at the polycrystalline Pt in hydrogen adsorption/desorption region arises from the employed preparation procedure.

In Fig. 1, the typical voltammograms recorded in the supporting electrolyte before and after Pt modification with adsorbed bismuth are compared. Distinctive characteristics for the presence of bismuth ad-atoms on the platinum surface are the diminution of the hydrogen adsorption/desorption charge due to the fact that hydrogen does not adsorb on Bi<sup>36</sup> and the appearance of peaks "a" and "a'", as a result of the irreversible oxidation/reduction of Bi adsorbed onto the Pt surface, which superimpose those corresponding to Pt oxide formation/reduction. Since only the Pt sites not blocked by Bi are available for hydrogen adsorption, the fractional coverage by Bi ad-atoms, evaluated from the decrease in charge involved in the hydrogen desorption before and after adsorption of Bi on the Pt electrode



surface, was set to be about 30 %, corresponding to the nominal content of Bi in the Pt<sub>2</sub>Bi catalyst.

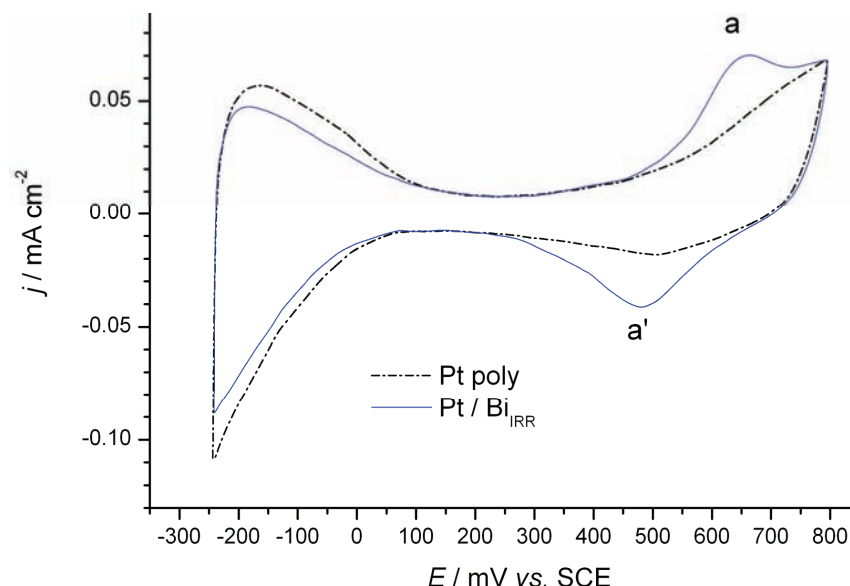


Fig. 1. Initial basic voltammograms for Pt/Bi<sub>irr</sub> and Pt catalysts in 0.1 M H<sub>2</sub>SO<sub>4</sub> solution.  
Scan rate: 50 mV s<sup>-1</sup>.

#### Oxidation of pre-adsorbed CO

Oxidation of pre-adsorbed CO was examined on Pt, Pt<sub>2</sub>Bi and Pt/Bi<sub>irr</sub> electrodes and the stripping voltammograms after subtraction of the background current are given in Fig. 2. As can be seen, the oxidation of CO<sub>ad</sub> started earlier on the Pt<sub>2</sub>Bi catalyst than on pure Pt. The difference in the onset and peak potential of CO<sub>ad</sub> oxidation could be ascribed to some electronic modification of the Pt surface atoms by Bi<sup>10,17,37,38</sup> resulting in weaker bonding of CO<sub>ad</sub>. This statement is consistent with literature data based on theoretical calculations.<sup>39,40</sup> However, the difference in onset and peak potentials between Pt/Bi<sub>irr</sub> and Pt catalysts was insignificant.

The CO stripping charge was also determined for the Pt<sub>2</sub>Bi electrode and corrected for the background currents to eliminate the contribution of the double layer charge, as well as Bi oxidation charge. Since Bi<sup>37</sup> and PtBi<sup>23,30</sup> are inactive for CO adsorption, the oxidation of CO occurs only on the Pt domains. Therefore, the charge under the CO<sub>ad</sub> peak at Pt<sub>2</sub>Bi reflects a process at the Pt parts and could be used for determining the contribution of pure Pt in the surface composition of Pt<sub>2</sub>Bi catalyst.<sup>35</sup>

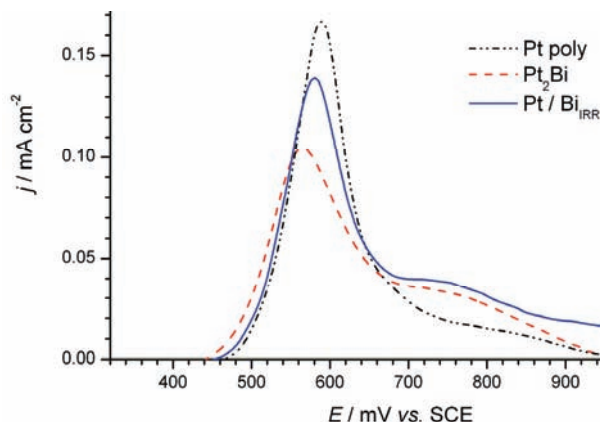


Fig. 2. CO stripping voltammograms on Pt<sub>2</sub>Bi, Pt/Bi<sub>IRR</sub> and Pt catalysts (first positive going sweeps) in 0.1 M H<sub>2</sub>SO<sub>4</sub> solution corrected for background current. Scan rate: 50 mV s<sup>-1</sup>.

#### Oxidation of formic acid

**Activity of the catalysts.** The activities of Pt<sub>2</sub>Bi, Pt/Bi<sub>IRR</sub> and Pt electrodes (first sweeps) towards formic acid oxidation are compared in Fig. 3. The cyclic voltammogram for the Pt electrode shows well established features for the oxidation of formic acid.<sup>8</sup> In the positive scan, the current slowly increased reaching a plateau at  $\approx 0.25$  V followed by ascending current starting at 0.5 V that attains a maximum at  $\approx 0.62$  V. This behavior could be explained by considering the dual path mechanism, *i.e.*, dehydrogenation assigned as the direct path, based on the oxidation of formate,<sup>41,42</sup> and dehydration, indirect path, assumes the formation of CO<sub>ad</sub>, both of which generate CO<sub>2</sub> as the final reaction product. At low potentials, HCOOH is oxidized through the direct path with the simultaneous formation of CO<sub>ad</sub>. Increasing coverage with CO<sub>ad</sub> reduces the number of Pt sites available for the direct path and the current slowly increases reaching a plateau. Subsequent formation of oxygen-containing species on the Pt enables the ox-

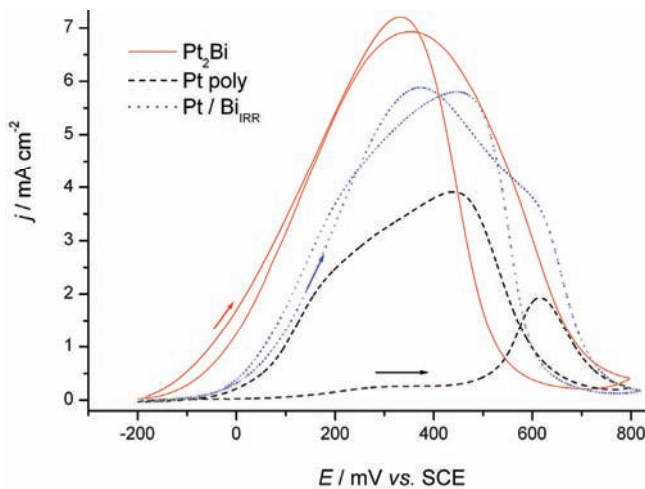


Fig. 3. Cyclic voltammograms for the oxidation of 0.125 M HCOOH in 0.1 M H<sub>2</sub>SO<sub>4</sub> solution on Pt, Pt<sub>2</sub>Bi and Pt/Bi<sub>IRR</sub> catalysts. Scan rate: 50 mV s<sup>-1</sup>.

dative removal of  $\text{CO}_{\text{ad}}$  and more Pt sites become available for  $\text{HCOOH}$  oxidation whereby the current increases until Pt oxide, inactive for  $\text{HCOOH}$  oxidation, is formed, which results in the current peak at  $\approx 0.62$  V. In the backward scan, the sharp increase of  $\text{HCOOH}$  oxidation current coincides with reduction of Pt oxide. The currents are much higher than in the forward sweep because the Pt surface is freed of  $\text{CO}_{\text{ad}}$ .

The polarization curves for bimetallic surfaces indicate a quite different behavior. Figure 3 shows that the onset potential for the reaction on  $\text{Pt}/\text{Bi}_{\text{irr}}$  was about 0.1 V less positive than on the Pt electrode. The current increases up to 0.35 V and reaches a peak, which corresponds to the oxidation of  $\text{HCOOH}$  to  $\text{CO}_2$  in the direct path, occurring on Pt sites that are not blocked by  $\text{CO}_{\text{ad}}$ . On the descending part of the curve, a shoulder appears at almost the same potential as the peak on the curve for the bare Pt electrode. The currents recorded in the backward direction are slightly higher, so the difference between forward and backward scan is not as large as on the bare Pt. Since the peak at  $\approx 0.62$  V arises from  $\text{HCOOH}$  oxidation on the Pt sites being freed by  $\text{CO}_{\text{ad}}$  oxidation, its height is an indication of the degree of Pt poisoning at lower potentials. Accordingly, the amount of  $\text{CO}_{\text{ad}}$  formed in the indirect path on  $\text{Pt}/\text{Bi}_{\text{irr}}$  is much lower than that formed on the pure Pt electrode.

The oxidation of formic acid on  $\text{Pt}_2\text{Bi}$  electrode starts at  $\approx -0.2$  V, which is 0.1 V less positive than on  $\text{Pt}/\text{Bi}_{\text{irr}}$  and  $\approx 0.2$  V less positive than on the Pt electrode. The current increases up to 0.35 V and reaches a peak about 15 times higher than the plateau on the curve for Pt. At more positive potentials, the reaction currents decrease due to surface oxide formation. The absence of a shoulder on the descending part of the curve, recorded on  $\text{Pt}/\text{Bi}_{\text{irr}}$ , indicating that no poisoning of the alloy by  $\text{CO}_{\text{ads}}$  occurred.

Well-shaped voltammogram clearly suggests that oxidation of  $\text{HCOOH}$  on  $\text{Pt}_2\text{Bi}$  proceeds through dehydrogenation path.<sup>35</sup> Since Bi does not adsorb  $\text{HCOOH}$ ,<sup>34,40</sup> oxidation of  $\text{HCOOH}$  occurs on the Pt sites in the pure Pt and Bi alloyed Pt domains. As is shown in Fig. 3, the lower activity of  $\text{Pt}/\text{Bi}_{\text{irr}}$  compared to  $\text{Pt}_2\text{Bi}$  and the appearance of a shoulder on the curve of  $\text{Pt}/\text{Bi}_{\text{irr}}$  could suggest a low coverage by  $\text{CO}_{\text{ad}}$  at the Pt sites on  $\text{Pt}/\text{Bi}_{\text{irr}}$ , *i.e.*, incomplete suppression of the dehydrogenation path although these two electrodes contained almost the same (nominal) amount of Bi. Thus,  $\text{HCOOH}$  oxidation on  $\text{Pt}/\text{Bi}_{\text{irr}}$  proceeded predominantly by the dehydrogenation path with some minor degree of dehydratation occurring as well. The increased selectivity toward the dehydrogenation path on  $\text{Pt}_2\text{Bi}$  as well as on  $\text{Pt}/\text{Bi}_{\text{irr}}$  compared to Pt was mainly the result of an ensemble effect caused by Bi reducing the continuous Pt sites necessary for dehydration. However, the ensemble effect on the  $\text{Pt}/\text{Bi}_{\text{irr}}$  catalyst was enabled by adsorbed Bi having practically no influence on the neighboring free Pt atoms. Whereas in the  $\text{Pt}_2\text{Bi}$  alloy, the ensembles were created by alloyed Bi atoms incorporated into



the Pt lattice, causing a shift in the d-band center of the adjacent Pt atoms. Therefore, Bi in the alloy also exhibited an electronic effect that could have been the reason for the better performance of this catalyst, resulting in higher currents and a lower onset potential.

*Stability of catalysts.* Cyclic voltammograms (first and 20<sup>th</sup> sweep) recorded on Pt<sub>2</sub>Bi and Pt/Bi<sub>irr</sub> catalysts in a formic acid containing solution are shown in Fig. 4. On potential cycling up to 0.8 V, the activity of the Pt<sub>2</sub>Bi electrode (Fig. 4a) slowly decreased during the first 5–7 cycles, reaching values of 90 and 82 % of the initial currents at the potential of the maximum current and at the potential of 0.0 V in the low current region, respectively. After these first few sweeps, the currents remain unchanged with further cycling (Inset in Fig. 4a). Since cycling of Pt<sub>2</sub>Bi in the supporting electrolyte leads to enhancement of the currents related to the oxidation of Bi species, indicating some surface decomposition caused by Bi leaching/dissolution processes,<sup>35</sup> the stability of Pt<sub>2</sub>Bi during oxidation of formic acid could be induced by the presence of HCOOH in the electrolyte. Abruna and co-workers<sup>43</sup> explained that the stability of Pt–Bi intermetallic surface originates from the competition between the oxidation of formic acid at the electrode/solution interface and Bi leaching, *i.e.*, corrosion/oxidation processes of the electrode surface itself. Accordingly, the main reason for high stability of formic acid oxidation current on the Pt<sub>2</sub>Bi catalyst was inhibition of the dehydration path, as well as, suppression of Bi leaching. This statement was confirmed by STM imaging before and after electrochemical treatment in formic acid-containing solution, which did not indicate any significant change of surface morphology and roughness after that procedure.<sup>35</sup>

Contrary to the Pt<sub>2</sub>Bi alloy, as can be seen in Fig. 4b, the Pt/Bi<sub>irr</sub> electrode showed significant changes with continuous cycling in a solution containing formic acid (Inset in Fig. 4b). Repetitive cycling up to 0.8 V shifted the onset potential for formic acid oxidation to more positive values, decreased the reaction currents, while anodic peak diminishes and a new peak starts to emerge and grow at ≈0.6 V. These transformations of the cyclic voltammograms indicate continuous Bi dissolution and modification of the surface composition. Upon prolonged cycling, the electrode surface became enriched in platinum and exhibited a Pt-like electrochemical behavior in the acid electrolyte containing formic acid. Apparently, re-adsorption of Bi species from the solution is rather low, so the initial voltammogram was never restored, which is in accordance with results obtained for formic acid oxidation on bismuth-coated mesoporous Pt microelectrodes.<sup>44</sup>

Finally, it could be concluded that the initial activities at the two Bi–Pt catalysts originate from the ensemble effect, but the activity of the Pt/Bi<sub>irr</sub> in the reaction is diminished due to leaching of Bi. An electronic effect contributes to the early start of the reaction on the alloy.



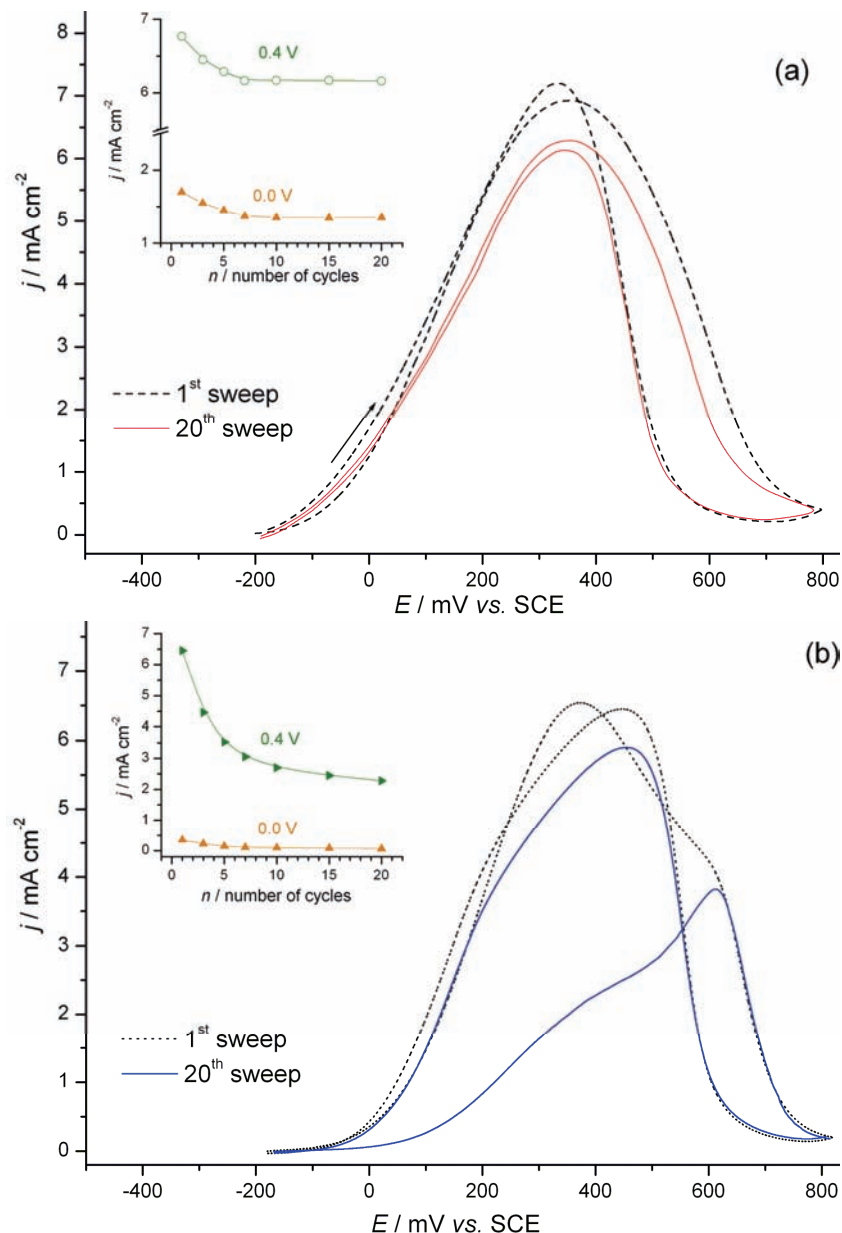


Fig. 4. First and 20<sup>th</sup> sweep for the oxidation of 0.125 M HCOOH in 0.1 M  $\text{H}_2\text{SO}_4$  solution on a)  $\text{Pt}_2\text{Bi}$  and b)  $\text{Pt}/\text{Bi}_{\text{irr}}$  catalysts. Insets: Effect of cycling – plots of the current density *vs.* number of cycles. Scan rate 50 mV s<sup>-1</sup>.

*Chronoamperometric measurements.* Chronoamperometric experiments were performed to prove the activity and stability of the investigated catalysts. The

current density of formic acid oxidation was recorded as a function of time at 0.20 V over 30 min (Fig. 5). The highest initial current density at 0.20 V on Pt<sub>2</sub>Bi compared to the other two catalysts is in accordance with the potentiodynamic measurements (Fig. 3). The initial currents at Pt<sub>2</sub>Bi electrode decreases slightly and in observed period of time attain a value which was about 3.5 times higher than at the Pt/Bi<sub>irr</sub> catalyst and almost 20 times higher than at the Pt electrode. The chronoamperometric results confirmed the high activity and stability of the Pt<sub>2</sub>Bi catalyst.

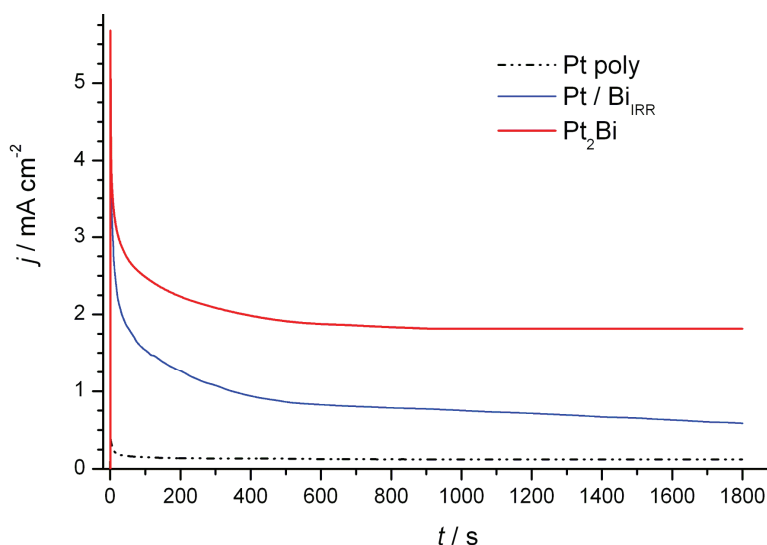


Fig. 5. Chronoamperometric curves for the oxidation of 0.125 M HCOOH at 0.20 V in 0.1 M H<sub>2</sub>SO<sub>4</sub> solution on Pt<sub>2</sub>Bi, Pt/Bi<sub>irr</sub> and Pt catalysts.

*Quasi-steady state measurements.* The results of the quasi-steady state measurements for formic acid oxidation at all the investigated electrodes are presented in Fig. 6. The data obtained under the slow sweep conditions corroborated the differences in the activities of pure Pt, Pt modified by Bi and Pt<sub>2</sub>Bi alloy that were found in the potentiodynamic measurements.

The Tafel slope on the Pt<sub>2</sub>Bi electrode was about 120 mV dec<sup>-1</sup>, indicating that the first electron transfer is the rate-determining step, with the transfer coefficient being about 0.5. This means that C–H bond cleavage, to form COOH<sub>ad</sub>, is the slow step and determines the rate of formic acid oxidation on Pt<sub>2</sub>Bi electrodes.

The Tafel slope of about 150 mV dec<sup>-1</sup> obtained during formic acid oxidation on bare Pt indicates that the formed CO was adsorbed and collected on the surface, thereby slowing down the reaction rate. The same value of Tafel slope was obtained for formic acid oxidation on carbon-supported high surface area

platinum.<sup>45</sup> A Tafel slope of 135 mV dec<sup>-1</sup> was found at Pt/Bi<sub>irr</sub>, which implies moderate surface coverage by CO<sub>ad</sub>.

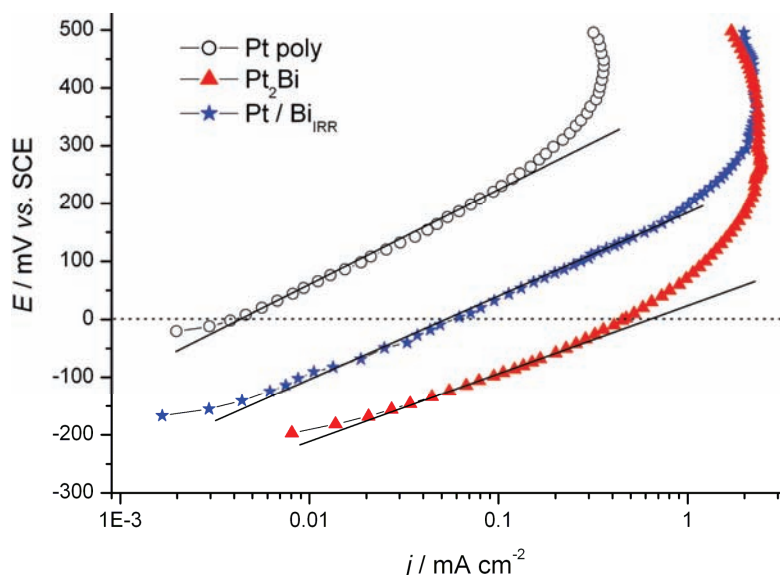


Fig. 6. Tafel plots for the oxidation of 0.125 M HCOOH in 0.1 M H<sub>2</sub>SO<sub>4</sub> solution on Pt<sub>2</sub>Bi, Pt/Bi<sub>irr</sub> and Pt catalysts. Scan rate: 1 mV s<sup>-1</sup>.

Comparing the activities of the investigated electrodes at 0.0 V, it can be seen that the current densities were enhanced 15 times at Pt/Bi<sub>irr</sub> and up two orders of magnitude at the Pt<sub>2</sub>Bi catalyst with respect to the Pt electrode.

#### CONCLUSIONS

Pt<sub>2</sub>Bi and Pt/Bi<sub>irr</sub> electrodes were investigated in the oxidation of formic acid and the results were compared to those of a Pt electrode. The presented results indicate that Bi in alloy and irreversibly adsorbed Bi exhibit different effects on the catalytic activity of these materials.

Pt<sub>2</sub>Bi is highly active for formic acid oxidation because the dehydrogenation path is predominant in the overall reaction. Bi in the alloy not only facilitates the ensemble effect, but also has an electronic effect that could be the reason for better performance of this catalyst, resulting in higher currents and a lower onset potential. The main reason for the high stability of the Pt<sub>2</sub>Bi catalyst is the inhibition of dehydration path in the reaction, as well as suppression of Bi leaching, indicated by the insignificant change in the surface morphology and roughness.

On the contrary, the Pt/Bi<sub>irr</sub> electrode was not stabilized by formic acid oxidation, since the desorption of Bi was not suppressed in the presence of formic acid, and a poisoning effect induced by the dehydration path was present. Since

$\text{Bi}_{\text{irr}}$  does not provoke any significant modification of the electronic environment, the modified Pt catalysts were less active than corresponding alloy.

Comparing the results obtained for these two Pt–Bi catalysts, the role of the ensemble effect and electronic effect in the oxidation of formic acid on Pt–Bi electrodes could be distinguished. The electronic effect, existing only on the alloy, contributes to an earlier start of the reaction, while the maximum current density is determined by the ensemble effect. During potential cycling of the Pt/ $\text{Bi}_{\text{irr}}$  electrode, Bi was leached from the electrode surface and the ensemble effect was reduced over time, or lost. Insight into the chronoamperometric curves confirmed the advantage of the alloys, *i.e.*, the necessity of alloying Pt with Bi to obtain a corrosion stable catalyst.

*Acknowledgement.* This work was financially supported by the Ministry of Education, Science and Technological development of the Republic of Serbia, Contract No. H-172060.

#### ИЗВОД

#### ЕЛЕКТРОКАТАЛИТИЧКА СВОЈСТВА Pt–Bi ЕЛЕКТРОДА У ОКСИДАЦИЈИ МРАВЉЕ КИСЕЛИНЕ

ЈЕЛЕНА Д. ЛОВИЋ, ДУШАН В. ТРИПКОВИЋ, КСЕНИЈА Ђ. ПОПОВИЋ, ВЛАДИСЛАВА М. ЈОВАНОВИЋ  
и АМАЛИЈА В. ТРИПКОВИЋ

ИХТМ – Центар за електрохемију, Универзитет у Београду, Његошева 12, Љ. др. 473, 11000 Београд

Оксидација мравље киселине испитивана је на два типа Pt–Bi катализатора:  $\text{Pt}_2\text{Bi}$  електроди и на поликристалној Pt електроди модификованијо иреверзibilno адсорбованим Bi ( $\text{Pt}/\text{Bi}_{\text{irr}}$ ). Активности су упређене са резултатима добијеним на чистој поликристалној Pt електроди. Циљ је био да се објасни разлика у деловању иреверзibilno адсорбованог Bi ( $\text{Bi}_{\text{irr}}$ ) и Bi у легираним стању. Показано је да су оба биметална катализатора активнија од поликристалне Pt, почетак реакције је померен ка негативнијим вредностима и у поређењу са чистом Pt при стационарним условима добијене су до два реда величине веће густине струје. Разлог за велику активност и стабилност  $\text{Pt}_2\text{Bi}$  електроде у оксидацији мравље киселине је одигравање реакције по главном рејону путу (дехидроганација мравље киселине), што је изазвано ефектом трећег тела и електронским ефектом, као и спречавање излуживања Bi из електроде. С друге стране, иако  $\text{Pt}/\text{Bi}_{\text{irr}}$  показује значајну почетну активност у односу на Pt, ова електрода није стабилна током реализације оксидације  $\text{HCOOH}$  због континуалног растварања Bi са површине електроде, као и тровања површине изазваног током реализације по индиректном, дехидратационом путу. Поређењем резултата добијених на ове две Pt–Bi електроде може се објаснити улога ефекта трећег тела и електронског ефекта у оксидацији  $\text{HCOOH}$ . Наиме, електронски ефекат, који постоји само код легуре, доприноси ранијем почетку реализације, док је максимална струја одређена ефектом трећег тела. Током циклизирања  $\text{Pt}/\text{Bi}_{\text{irr}}$  електроде Bi одлази са површине и ефекат трећег тела се губи током времена. Хроноамперометријска мерења указују на предност легуре, односно неопходност легирања Bi са Pt да би се добио корозионо стабилан катализатор.

(Примљено 12. октобра, ревидирано 16. новембра 2012)

## REFERENCES

1. R. Parsons, T. Vander Noot, *J. Electroanal. Chem.* **257** (1988) 9
2. A. V. Tripković, J. D. Lović, K. Dj. Popović, *J. Serb. Chem. Soc.* **75** (2010) 1559
3. J. D. Lović, K. Dj. Popović, A. V. Tripković, *J. Serb. Chem. Soc.* **76** (2011) 1523
4. S. Stevanović, D. Tripković, D. Poleti, J. Rogan, A. Tripković, V. M. Jovanović, *J. Serb. Chem. Soc.* **76** (2011) 1673
5. X. Xia, T. Iwasita, *J. Electrochem. Soc.* **140** (1993) 2559
6. X. Wang, J.-M. Hu, I.-M. Hsing, *J. Electroanal. Chem.* **562** (2004) 73
7. A. V. Tripković, K. Đ. Popović, J. D. Lović, *J. Serb. Chem. Soc.* **68** (2003) 849
8. A. Capon, R. Parsons, *J. Electroanal. Chem.* **44** (1973) 1
9. J. M. Feliu, E. Herrero, *Formic acid oxidation*, in *Handbook of Fuel Cells-Fundamentals Technology and Applications*, Vol. 2, W. Vielstich, A. Lamm, H. A. Gasteiger, Eds., Wiley, New York, 2003, Ch. 42, p. 625
10. E. Herrero, A. Fernandez-Vega, J. M. Feliu, A. Aldaz, *J. Electroanal. Chem.* **350** (1993) 73
11. J. Clavilier, A. Fernandez-Vega, J. M. Feliu, A. Aldaz, *J. Electroanal. Chem.* **258** (1989) 89
12. J. Clavilier, A. Fernandez-Vega, J. M. Feliu, A. Aldaz, *J. Electroanal. Chem.* **261** (1989) 113
13. B.-J. Kim, K. Kwon, C. K. Rhee, J. Han, T.-H. Lim, *Electrochim. Acta* **53** (2008) 7744
14. A. Sáez, E. Expósito, J. Solla-Gullón, V. Montiel, A. Aldaz, *Electrochim. Acta* **63** (2012) 105
15. A. Lopez-Cudero, F. J. Vidal-Iglesias, J. Solla-Gullon, E. Herrero, A. Aldaz, J. M. Feliu, *Phys. Chem. Chem. Phys.* **11** (2009) 416
16. J. Clavilier, J. M. Feliu, A. Aldaz, *J. Electroanal. Chem.* **243** (1988) 419
17. J. Kim, C. K. Rhee, *Electrochim. Comm.* **12** (2010) 1731
18. Q.-S. Chen, Z.-Y. Zhou, F. J. Vidal-Iglesias, J. Solla-Gullon, J. M. Feliu, S.-G. Sun, *J. Am. Chem. Soc.* **133** (2011) 12930
19. C. Jung, T. Zhang, B.-J. Kim, J. Kim, C. K. Rhee, T.-H. Lim, *Bull. Korean Chem. Soc.* **31** (2010) 1543
20. D. Volpe, E. Casado-Rivera, L. Alden, C. Lind, K. Hagerdon, C. Downie, C. Korzniewski, F. J. DiSalvo, H. D. Abruna, *J. Electrochem. Soc.* **151** (2004) A971
21. E. Casado-Rivera, D. J. Volpe, L. Alden, C. Lind, C. Downie, T. Vazquez-Alvarez, A. C. D. Angelo, F. J. DiSalvo, H. D. Abruna, *J. Am. Chem. Soc.* **126** (2004) 4043
22. H. Wang, L. Alden, F. J. DiSalvo, H. D. Abruna, *Phys. Chem. Chem. Phys.* **10** (2008) 3739
23. M. Oana, R. Hoffmann, H. D. Abruna, F. J. DiSalvo, *Surf. Sci.* **574** (2005) 1
24. C. Roychowdhury, F. Matsumoto, V. B. Zeldovich, S. C. Warren, P. F. Mutolo, M. J. Ballesteros, U. Wiesner, H. D. Abruna, F. J. DiSalvo, *Chem. Mater.* **18** (2006) 3365
25. Y. Liu, M. A. Lowe, F. J. DiSalvo, H. D. Abruna, *J. Phys. Chem., C* **114** (2010) 14929
26. L. M. Magno, W. Sigle, P. A. van Aken, D. G. Angelescu, C. Stubenrauch, *Chem. Mater.* **22** (2010) 6263
27. X. Yu, P. G. Pickup, *Electrochim. Acta* **56** (2011) 4037
28. Y. Liu, M. A. Lowe, K. D. Finkelstein, D. S. Dale, F. J. DiSalvo, H. D. Abruna, *Chem. Eur. J.* **16** (2010) 13689.
29. X. Ji, K. T. Lee, R. Holden, L. Zhang, J. Zhang, G. A. Botton, M. Couillard, L. F. Nazar, *Nat. Chem.* **2** (2010) 286
30. E. Casado-Rivera, Z. Gal, A. C. D. Angelo, C. Lind, F. J. DiSalvo, H. D. Abruna, *ChemPhysChem* **4** (2003) 193
31. N. de-los-Santos-Alvarez, L. R. Alden, E. Rus, H. Wang, F. J. DiSalvo, H. D. Abruna, *J. Electroanal. Chem.* **626** (2009) 14



32. I. Pašti, S. Mentus, *Phys. Chem. Chem. Phys.* **11** (2009) 6225
33. D. R. Blasini, D. Rochefort, E. Fachini, L. R. Alden, F. J. DiSalvo, C. R. Cabrera, H. D. Abruna, *Surf. Sci.* **600** (2006) 2670
34. A. V. Tripković, K. Dj. Popović, R. M. Stevanović, R. Socha, A. Kowal, *Electrochem. Comm.* **8** (2006) 1492
35. J. D. Lović, M. D. Obradović, D. V. Tripković, K. Dj. Popović, V. M. Jovanović, S. Lj. Gojković, A. V. Tripković, *Electrocatalysis* **3** (2012) 346
36. R. Gomez, J. M. Feliu, A. Aldaz, *Electrochim. Acta* **42** (1997) 1675
37. T. J. Schmidt, B. N. Grgur, R. J. Behm, N. M. Markovic, P. N. Ross, Jr., *Phys. Chem. Chem. Phys.* **2** (2000) 4379
38. B. E. Hayden, A. J. Murray, R. Parsons, D. J. Pegg, *J. Electroanal. Chem.* **409** (1996) 51
39. L.-L. Wang, D. D. Johnson, *J. Phys. Chem., C* **112** (2008) 8266
40. N. Kapur, B. Shan, J. Hyun, L. Wang, S. Yang, J. B. Nicholas, K. Cho, *Mol. Simul.* **37** (2011) 648
41. A. Miki, S. Ye, M. Osawa, *Chem. Commun.* (2002) 1500
42. G. Samjeske, A. Miki, S. Ye, M. Osawa, *J. Phys. Chem., B* **110** (2006) 16559
43. Y. Liu, M. A. Lowe, F. J. DiSalvo, H. D. Abruna, *J. Phys. Chem., C* **114** (2010) 14929
44. S. Daniele, C. Bragato, D. Battistel, *Electroanalysis* **24** (2012) 759
45. J. D. Lović, A. V. Tripković, S. Lj. Gojković, K. Dj. Popović, D. V. Tripković, P. Olszewski, A. Kowal, *J. Electroanal. Chem.* **581** (2005) 294.

